Morphogenesis of *Doublefoot* (*Dbf*), a mouse mutant with polydactyly and craniofacial defects

CHRISTOPHER HAYES[1], MARY F. LYON[2] AND GILLIAN M. MORRISS-KAY[1]

[1] *Department of Human Anatomy, University of Oxford, and* [2] *MRC Mammalian Genetics Unit, Harwell, UK*

(*Accepted 30 March 1998*)

ABSTRACT

We report the morphogenesis of a new mouse mutant, *Doublefoot* (*Dbf*). The major phenotypic features involve the limb and craniofacial regions. There is polydactyly of all 4 limbs, with typically 6–8 digits per limb. All of the digits are triphalangeal; some show bifurcations and some are not attached to the carpus/tarsus. The carpus and tarsus are broader than normal, and their elements are partially fused. There are also tibial defects. Mutant embryos show a diencephalic bulge on d 10.0, with older animals exhibiting broadened and bulbous skulls sometimes with an additional midline skeletal element, shortened snouts and bulging eyes. Homozygotes, which do not survive beyond d 15, show midline facial clefting. In this study of the embryonic and fetal development of *Dbf* animals, we focus on the morphogenesis of the limbs and head, and discuss the possible molecular developmental mechanisms.

Key words: Limb development; *Sonic hedgehog*.

INTRODUCTION

The vertebrate limb has long been used by experimental embryologists as a paradigm to elucidate the myriad complex cellular interactions involved in the generation of various types of differentiated cells and tissues during embryonic development. The advantage of using spontaneous or induced mutants, rather than mice with the targeted disruption of a defined genetic locus, is that mutants can be selected for study on the basis of a specific phenotype. This allows the investigator to analyse the processes, both genetic and morphogenetic, that generate the mutant phenotype, and to gain new information about the rules governing normal development.

The murine forelimb bud first becomes visible late on d 9 of gestation, as a mesenchymal outgrowth of the embryonic lateral plate mesoderm encased by undifferentiated ectodermal cells. About half a day later the hindlimb bud becomes apparent; its development is consistently behind that of the forelimb. As outgrowth of the limb continues, its development can be described with reference to the 3 cartesian axes, which in the upper limb are: the proximodistal (PD) axis that runs from the shoulder to the extremities of the digits; the anteroposterior (AP) axis from digit I (thumb) to digit V (little finger); and the dorsoventral (DV) axis, from the back of the hand to the palm of the hand.

Around d 10 the murine limb becomes rimmed by an epithelial thickening, the apical ectodermal ridge (AER). The AER is the source of signals responsible for maintaining limb bud outgrowth; extirpation results in truncations of the limb in a stage-dependent manner (Saunders, 1948; Summerbell et al. 1973). A major function of the AER is to maintain the underlying mesenchyme in a proliferative and undifferentiated state: this function depends on its secretion of fibroblast growth factors (Savage et al. 1993; Niswander et al. 1994). This proliferating distal mesenchyme is termed the progress zone (PZ). It is thought that as cells progressively leave the PZ they form progressively more distal elements of the limb, accounting for the proximodistal specification of the skeletal elements of the limb (Saunders, 1948; Summerbell et al. 1973).

Correspondence to Professor Gillian M. Morriss-Kay, Department of Human Anatomy, University of Oxford, South Parks Road, Oxford OX1 3QX, UK.

The zone of polarising activity (ZPA) is a morphologically indistinct region of posterodistal mesenchyme; it is the source of signals which pattern the anteroposterior (AP) axis of the limb. The ZPA was discovered by classical transplantation studies in chick embryos and defined as a region of posterior limb mesenchyme which has the ability to induce mirror-image duplications when grafted to the anterior border of a chick wing (Saunders & Gasseling, 1968).

We describe here the morphogenesis of a new mouse mutant *Doublefoot* (*Dbf*). The phenotype is due to a single mutant gene, which is inherited in a dominant manner (Lyon et al. 1996*a*). Homozygotes are not recovered beyond the fifteenth day of gestation. Heterozygotes show reduced viability and fertility. The study of mutants such as *Dbf* has the potential to reveal new information concerning the interactions involved in morphogenesis of the limbs and head. The many dysmorphic syndromes involving both regions, and the analysis of gene expression patterns during limb and craniofacial development, show that these 2 regions share common signalling systems (reviewed by Winter 1994). This study forms the morphogenetic basis of a detailed analysis of the molecular mechanisms underlying abnormal limb and craniofacial development, part of which is reported elsewhere (Hayes et al. 1998).

MATERIALS AND METHODS

Mice

F1 hybrids from a C3H and 101 cross were mated with *Dbf* mice; wild type mice were C3H/101 hybrids. Animals were housed under standard conditions in the animal facilities in Oxford and Harwell. Pregnant dams (day of vaginal plug designated d 0) were killed by cervical dislocation and their uteri dissected into sterile Tyrode's saline. Embryos were dissected free from the uterus and extra-embryonic membranes using watchmakers' forceps under a dissecting microscope. For convenience all mutant animals are referred to as *Dbf* in the text irrespective of genotype, unless specifically stated. At least 2 litters were examined for external appearance at each stage. For skeletal analysis, at least 4 litters were examined.

Skeletal staining and histology

Embryos and fetuses up to d 15 were fixed in Bouin's fixative overnight, halved sagittally and washed in distilled water. Cartilage staining was performed as described by Watson (1977) and samples were cleared and stored in 3 parts methyl salicylate to 1 part benzyl benzoate. Fetuses over 17 d and newborn pups were fixed overnight in 95% alcohol and stained according to Watson (1977), with the addition of 1% alizarin red after maceration in KOH; they were cleared in increasing concentrations of glycerine/70% alcohol/water and stored in 100% glycerine. For histology, Bouin's-fixed samples were dehydrated and embedded in paraffin and 7 μm sections cut and mounted. They were stained with haematoxylin and eosin (H&E).

RESULTS

Morphological examination of mutant animals

Dbf mice can be distinguished from their normal littermates on d 10 of gestation by the presence of a midline bulge in the roof of the diencephalon (Fig. 1*a*). At this stage the mutant animals have no other discernible phenotypic features. Late on d 10 the mutant limbs can be seen to be enlarged slightly along the AP axis. By d 11 of gestation the enlarged limbs of the *Dbf* animals are easily distinguishable from those of their normal littermates, and the diencephalic bulge persists (Fig. 2*a*, *b*).

By d 12 the hand- and footplates of the mutant animals are greatly enlarged along the anteroposterior axis, with the enlargement exclusively on the preaxial (anterior) aspect of the limb, no difference being detectable between the postaxial (posterior) margins of the mutant and wild type limbs (Fig. 2*c*, *d*). At this stage the distal limb margin of the normal and mutant animals has taken on the characteristic angular appearance that precedes the formation of discrete digital condensations. On d 13 the blastemata of the 5 digits are clearly distinguishable in wild type limb buds (Fig. 3*a*); in contrast, the limbs of the *Dbf* mice show the condensing models for more than 5 digits (Fig. 3*b*). At this stage *Dbf* embryos are smaller than their normal littermates; this difference persists throughout life. The craniofacial region of mutant d 13 embryos is much more bulbous than that of wild type littermates, with the characteristic midline cleft apparent in homozygous animals (Fig. 3*c*, *d*). The length of *Dbf* limbs is normal at this stage and at all subsequent stages.

At d 14 digital separation is advanced in the normal limb, whereas the interdigital web still persists in some of the *Dbf* limbs. Some of the mutant limbs show putative interdigital mesenchymal condensations (Fig. 4*b*). At d 15, the digits of the normal limb are clearly separate, but in the mutant limbs some of the digits

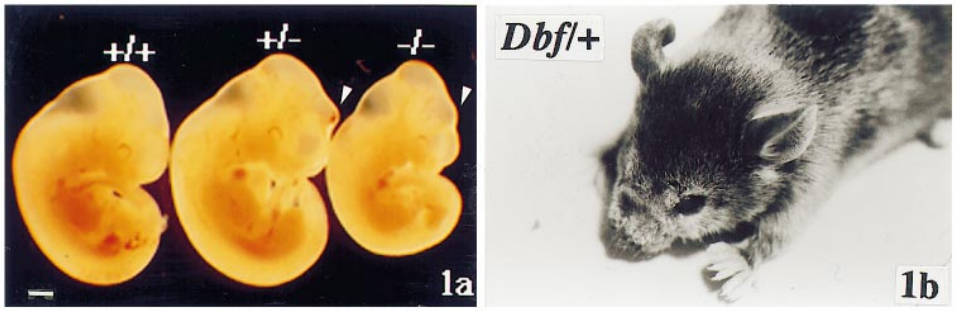

Fig. 1. (*a*) Appearance of d 10.5 living embryos, genotypes as indicated; arrows indicate the diencepalic bulge present in the mutant embryos. Bar = 500 μm. (*b*) Eight-week old heterozygous animal, showing polydactylous limbs and bulbous forehead.

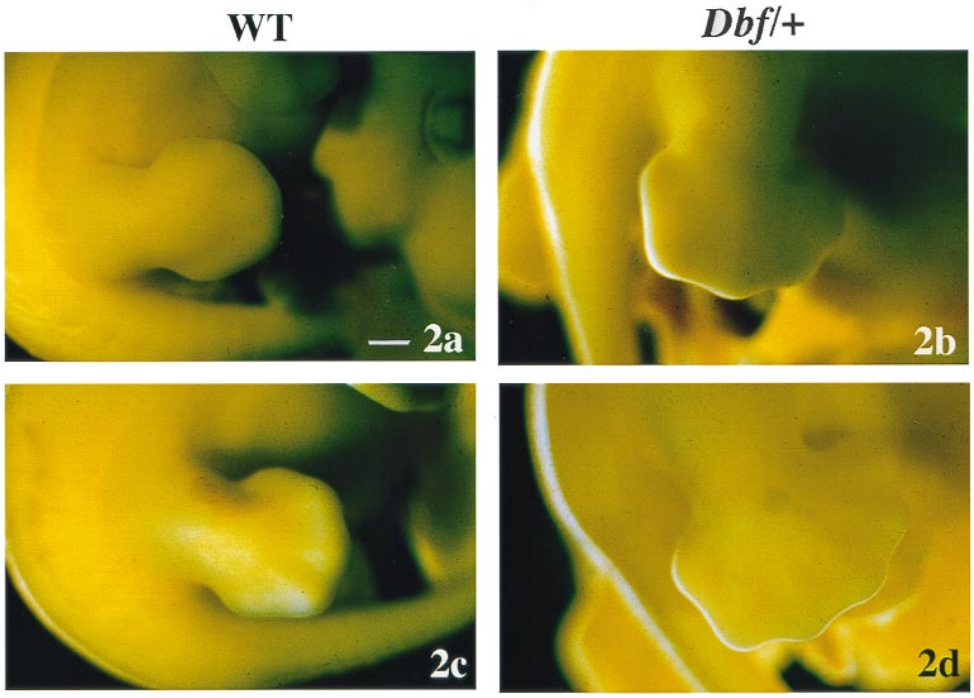

Fig. 2. (*a*) Day 11 wild type limb and (*b*) *Dbf*/+ limb of the same age clearly enlarged along the anteroposterior axis. (*c*) Day 12 wild type limb and (*d*) *Dbf*/+ limb showing blastemata for the condensing digits. Bar, 100 μm.

are still joined due to incomplete loss of the interdigital mesenchyme.

Examination of d 17 fetuses clearly shows that some of the limbs are polysyndactylous. *Dbf* mice can be easily distinguished at birth by the presence of broad paws with a fan-shaped array of digits and abnormal orientation of the hindlimbs. This hindlimb abnormality is a characteristic feature of this mutant, with all the adult mice having a talipes equinovarus deformity (clubfoot); the feet are held so that the animals walk on the outer border of their feet, and in extreme cases the foot is dorsiflexed to such an extent that the animals walk on the outer border of the ankle. Some adult animals also show a slight rotational defect of the forefoot, which is apparent as early as d 13 (compare forelimbs in Fig. 3*c*, *d*). The cranium is abnormally bulbous, with a broadened snout. The tails of the mutant mice are also markedly kinked (Fig. 7*a*, *b*).

Examination of the skeletal pattern of mutant embryos and fetuses

The cartilaginous skeletal patterns of d 14 and 15 embryos were visualised by Alcian blue staining on fixed, halved embryos (Fig. 4). At d 14 the polydactylous digital pattern is apparent, with the *Dbf* limbs having a fan-like appearance (compare Fig. 4*a*, *c* with *b*, *d*). All the digits are the same length; in addition, some of the limbs have bifuricated digits.

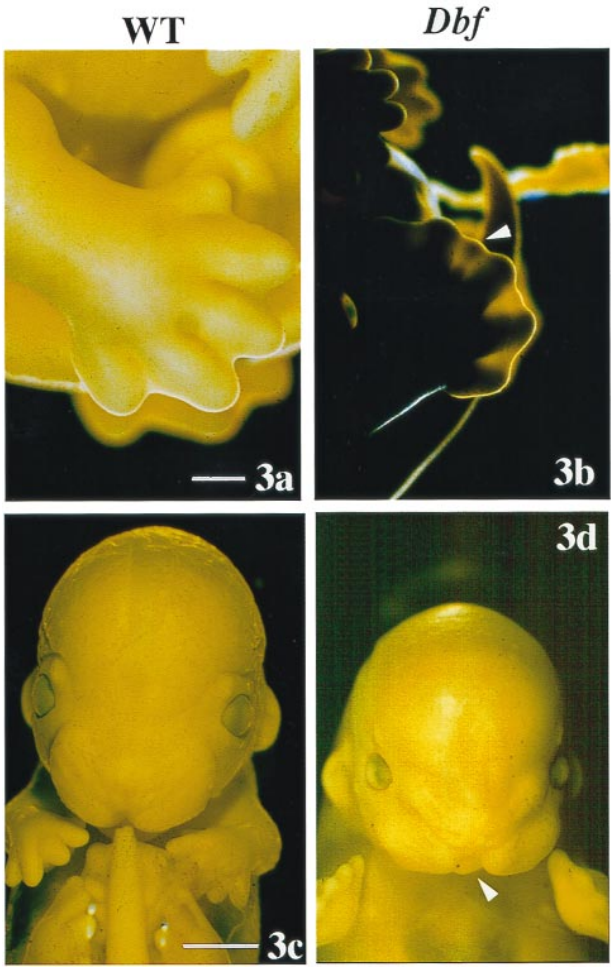

Fig. 3. (*a*) Day 13 wild type limb; (*b*) *Dbf*/+ limb showing preaxial polydactyly; the sample is backlit to show an ectopic interdigital element (arrowed). (*c*) Day 13 wild type face and (*d*) *Dbf*/*Dbf* face; the homozygous mutant head is more bulbous than that of the wild type, and shows the characteristic midline cleft (arrow); note also the dorsoventral thickening of the hand plates. Bars: *a*, *b*, 100 μm; *c*, *d*, 500 μm.

The interdigital condensations detected prior to skeletal staining can be seen to be unconnected to the future carpus or tarsus (Fig. 4*b*). Examination of the more proximal limb bones revealed that the tibia has separate proximal and distal sites of chondrogenesis.

By d 15 the most notable feature of the *Dbf* limbs is the lack of any anteroposterior polarity, with none of the digits resembling a pollex or hallux (digit I) (Fig. 4*e–h*). Digit I is characterised by 2 phalanges, compared with 3 phalanges in the other digits; all of the mutant digits are triphalangeal. In some cases, the most anterior digit was bifid. The digits showed a greater separation, especially distally, than those of wild type limbs (Fig. 4*c*, *d*). Closer examination of the carpus and tarsus of these animals revealed that the carpal and tarsal elements were duplicated to the same extent as the digits. In the carpus and tarsus of the normal limb, discrete and distinguishable elements can be identified at this stage, whereas in the mutant limb the carpus and tarsus consist of 2 rows of morphologically indistinct, contiguous elements (Fig. 4*g*, *h*).

Examination of the tibia and fibula revealed that the distal portion of the tibia curves helically about its longtitudinal axis, giving it an almost 'corkscrew' appearance (Fig. 4*g*, *h*). The curved shape results from the fusion of separate proximal and distal cartilages that are not aligned with each other. The fibula appears to articulate normally with the anterior head of the talus, but the distal end of the tibia makes an incomplete, medially situated articulation. The corresponding bones of the forelimb, the radius and ulna, are normal (Fig. 4*e*, *f*), as are the other components of the cartilaginous skeleton (not shown).

At d 17, by which stage only heterozygous fetuses survive, the cartilage models have begun to ossify and the membrane bones of the skull are well developed. Double-stained skeletal preparations of the appendicular parts of the skeleton reveal that the timing of ossification in *Dbf* fetuses is entirely normal, suggesting that the phenotype is not due to heterochrony (perturbation in the timing) in the *Dbf* mice (Fig. 5*a–d*). The only other abnormal feature noted in some of the mutant forelimbs was the presence of a scapular hole on the supraspinuous fossa of the scapula (Fig. 1 of Hayes et al. 1998). When present, this defect was always unilateral and was never seen in animals beyond E17, suggesting that the hole is temporary and does not hinder the subsequent development of a completely ossified, morphologically normal scapula. Each of the mutant limbs supports at least 6 triphalangeal digits, with a maximum of 9, including interdigital digits and bifurcated digits. The precise pattern and number of digits varies from limb to limb as well as from animal to animal; approximately 1 in 8 limbs shows an interdigital digit, and approximately 1 in 4 shows bifurcation. (Interdigital and bifurcated digits at this stage are illustrated in Hayes et al., 1998.) The hindfeet are medially rotated, due to the hypoplastic tibia juxtaposed with the relatively normal fibula, and abnormal articulation of the tibia with the foot (Fig. 5*c*, *d*), in virtually all mutant limbs. The bowing of the fibula appears to be due to the shorter tibia, to which it becomes fused in the mouse. Postpartum animals show all of the features seen at d 17; although rare, a rotational defect of the radius is sometimes observed (Fig. 5*e*, *f*).

In d 17 and newborn pups the membrane bones of the cranium have formed; those of mutant pups show the normal reticular appearance. The most notable

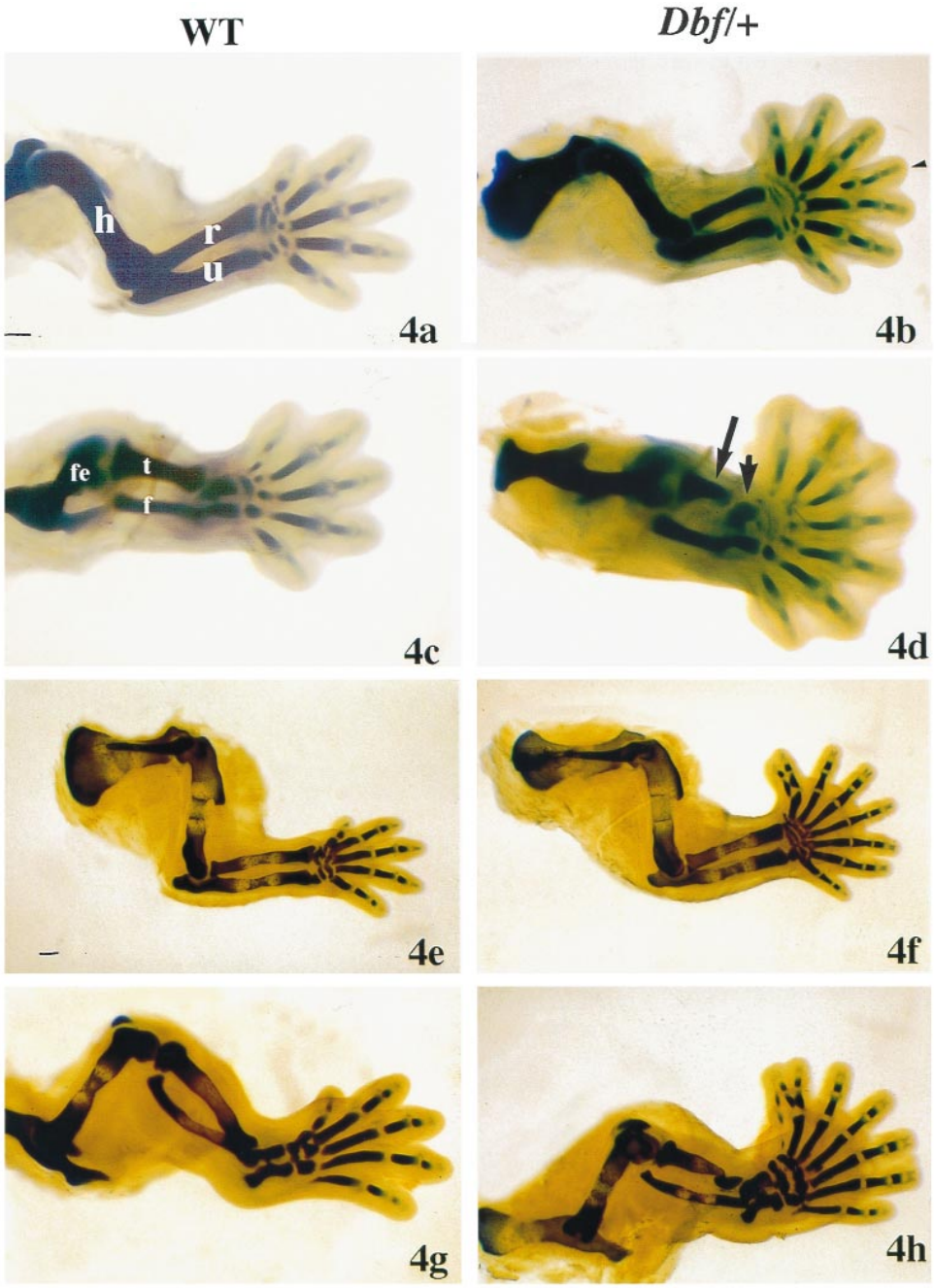

Fig. 4. Cartilaginous skeletons of d 14 forelimbs (*a*, *b*) and hindlimbs (*c*, *d*) and d 15 forelimbs (*e*, *f*) and hindlimbs (*g*, *h*), wild type and *Dbf/+* as indicated. A cartilaginous interdigital element is shown in (*b*) (arrowhead); partial duplication of the first digit is shown in (*f*) and (*h*); (*h*) also shows a chain of cartilaginous elements anterior to the first digit. The *Dbf/+* tibia forms from separate proximal and distal cartilaginous condensations (arrowed in *d*) which fuse at d 15 (*h*) but are poorly aligned. h, humerus, r, radius, u, ulna, fe, femur, t, tibia, f, fibula. Bar, 100 μm.

feature of the skulls is that the frontal and parietal bones are separated by wider than normal metopic and sagittal sutures (Fig. 6*c*, *d*). In some, a supernumerary element (wormian bone) is present in the anterior fontanelle of the mutant skull (Fig. 6*c*). Shape of the individual calvarial bones is variable, but the overall effect is a broader and more bulbous skull (Fig. 6*c*, *d*). In the postpartum animals the tails are frequently kinked (Fig. 7*b*); the skeletal preparations reveal, in accordance with the observations of Lyon et al. (1996*a*), that the underlying defect is not osseous. Although the rest of the skeleton is relatively normal, there are some minor abnormalities or variations, including a slightly compressed ribcage and a smaller cervical-cranial angle (Fig. 7*a*, *b*); these specimens also illustrate the different limb positions.

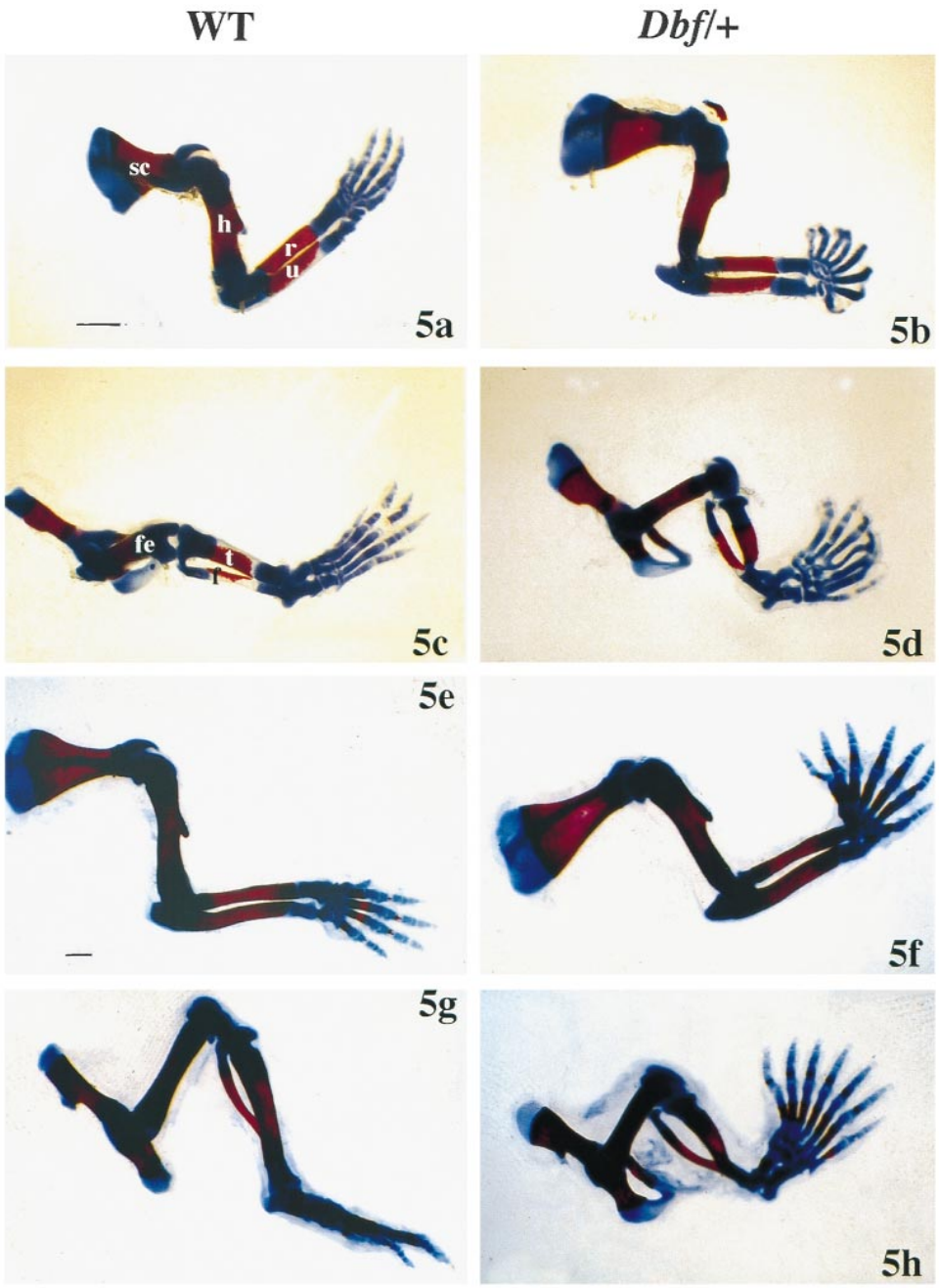

Fig. 5. Double-stained skeleton of d 17 (*a*) wild type forelimb and (*b*) *Dbf*/+ forelimb; (*c*) wild type hindlimb and (*d*) *Dbf*/+ hindlimb. Skeleton of newborn (*e*) wild type forelimb and (*f*) *Dbf*/+ forelimb; (*g*) wild type hindlimb and (*h*) *Dbf*/+ hindlimb showing bowing of the fibula alongside the abnormal tibia, and the rotational deformity of the hindlimb. sc, scapula, h, humerus, r, radius, u, ulna, fe, femur, t, tibia, f, fibula. Bar, 500 μm.

Histological analysis

Day 13 limbs were removed and embedded in paraffin and stained with H & E to examine the histology of the developing mutant limbs. Because the condensing digits of *Dbf* limbs do not all develop in the same plane, some of the condensations lie either slightly dorsally or slightly ventrally with respect to the main digital plane (Fig. 8*a*, *b* and *e*, *f*). Some sections also reveal the presence of condensations in the interdigital mesenchyme, which in normal embryos do not give rise to a digit (Fig. 8*a*, *b*). These condensations are of 2 types, both of which are seen in the skeletal preparations: (a) full length digits corresponding to the interdigital condensations seen in whole embryos, which are not connected to the carpus or tarsus (Fig. 4*b*), and (b) small nodules of cartilage (Fig. 4*f*). A remnant of the AER which has failed to regress is present in the ectoderm overlying both types of supernumerary condensation (Fig. 8*c*, *d*). In normal

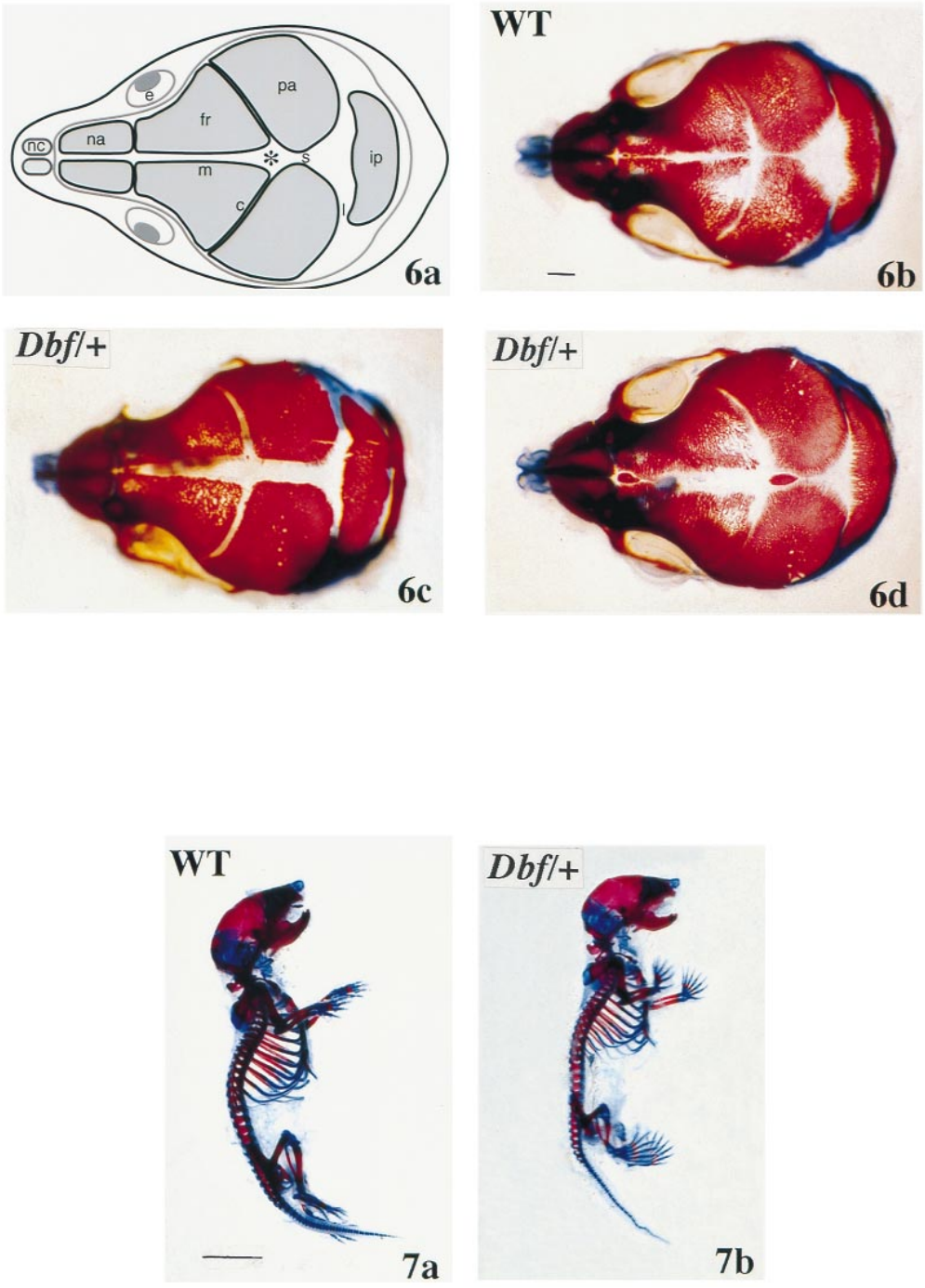

Fig. 6. (*a*) Diagram showing the calvarial bones and sutures of the skull. na, nasal bones; nc, nasal cartilage; fr, frontal bones; pa, parietal bones; ip interparietal bone; m, metopic suture; c, coronal suture; s, sagittal suture; l, lambdoid suture; asterix, anterior fontanelle. Newborn skull vaults of (*b*) wild type, (*c*) *Dbf*/+ skull, showing widened sutures, (*d*) *Dbf*/+ skull showing an additional (wormian) bone in the anterior fontanelle (asterisk). A small wormian bone is also present in the metopic sutures of the wild type skull (*b*). Bar, 500 μm.

Fig. 7. Skeletons of (*a*) wild type and (*b*) *Dbf* pups: note the compression of the ribcage, the angle of the head, and the orientation of the feet. Bar, 5 mm.

d 13 limbs the AER has completely regressed from the interdigital regions, persisting only at the tips of the developing digits (not shown).

Histological analysis also confirmed that the mutant limbs are much thicker dorsoventrally than their wild type counterparts (Fig. 8*e*, *f*; see also Fig. 3*c*, *d*). This feature is secondary to the formation of the extra digits, since the digital plates of *Dbf* limbs are enlarged along the AP axis before the limbs have enlarged along the DV axis. The mesenchyme of the *Dbf* limbs is not as well organisied as that of normal limbs, with a larger volume of extracellular matrix compared to

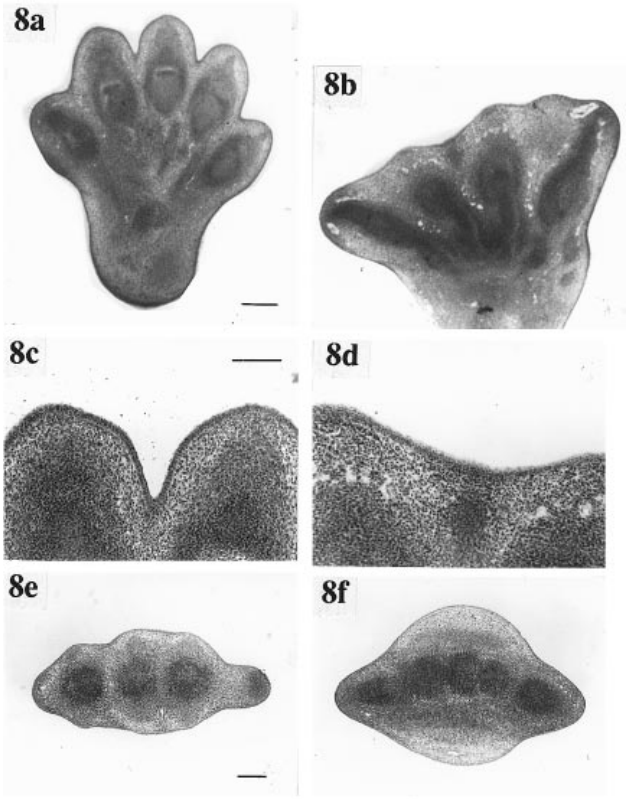

Fig. 8. Sections of d 13 forelimbs: (*a*, *c*, *e*) wild type; (*b*, *d*, *f*) *Dbf*/+, cut in the plane of the handplate (*a–d*), or transversely (*e*, *f*). The *Dbf*/+ limbs show an interdigital condensation (arrowed in *b*, *d*) and dorsoventral thickening due to excessive mesenchymal proliferation (*f*). The plane is curved in (*f*), restricting the number of digits that can be seen in the horizontal plane (*b*). *a*, *b*, *e*, *f*, 100 μm; *c*, *d*, 500 μm.

normal limbs of the same age (Fig. 8 *a*, *b* and *e*, *f*). In older animals this soft tissue defect persists, with mutant limbs having a characteristically enlarged ventral footpad. The soft tissue of the tail in *Dbf* animals is much thicker than that of their normal siblings.

DISCUSSION

Here we report the morphogenesis of a new mouse mutant, *Dbf*, which is characterised phenotypically by polydactyly and craniofacial abnormalities. Mutants are phenotypically distinguishable on d 10.0 by the presence of a diencephalic bulge; by d 10.5 to early d 11.0 the limb buds of mutant animals are clearly enlarged along the anteroposterior axis, with the extra tissue located preaxially. Development of the cranium is also perturbed by the *Dbf* mutation, indicating a common mechanism in the genesis of the limb and craniofacial defects. Interestingly, these 2 areas share common signalling molecules (Wilkie et al. 1995), and several human dysmorphogenesis syndromes affecting the development of both structures have also been noted (Winter, 1994; Wilkie et al. 1995).

The *Dbf* limb phenotype is fully penetrant but exhibits variable expressivity: all mutant limbs are polydactylous, with the extent of the polydactyly varying from mouse to mouse, and from limb to limb within the same mouse. Digital bifurcations were seen in approximately 1 in 4 limbs, and interdigital elements in approximately 1 in 8 limbs. The mutants exhibit not only polydactyly, defined as duplication of the digital elements, but appropriately exhibited diplocheiria and diplopodia of the fore- and hindlimbs, defined as the duplication of some of the carpal and tarsal elements in addition to the digits (Karchinov, 1973). The anteriormost digit was invariably triphalangeal, and therefore could not be characterised as a pollex or hallux. In other mouse mutants with preaxial polydactyly, the limbs can be characterised as having partial mirror-image duplications (Masuya et al. 1997). In contrast, *Dbf* limbs are not mirror-image, but harbour an array of identical triphalangeal digits.

The uniform feature of all polydactylous limb buds is that they are larger than normal limbs along the anteroposterior axis (Tickle & Eichele, 1994). We suggest that supernumerary digital condensations form when the excess tissue surpasses a threshold level. This is supported by the finding that in some limbs small cartilaginous interdigital nodules are formed, rather than complete identifiable digits; we suggest that these nodules form where mesenchymal proliferation has exceeded the threshold level, but there is not sufficient tissue present to form a complete digit. Complete (triphalangeal) digits were also observed interdigitally, suggesting a greater degree of proliferation of the interdigital mesenchyme at these sites. Interdigital proliferation is inhibited in normal limbs by loss of the AER. In *Dbf* the AER fails to regress from the interdigital spaces, allowing the persistence of mitogenic signals to the underlying mesenchyme, creating an excess of interdigital tissue which subsequently forms the ectopic interdigital condensations.

Interdigital chondrogenesis has been induced experimentally in avian embryos by removal of the interdigital ectoderm (Hurle et al. 1989). Normally, interdigital chondrogenesis is inhibited by the close proximity of the 2 layers of ectoderm, each of which has an inhibitory influence on chondrogenesis mediated by hyaluronan-rich extracellular matrix in the subectodermal layers (Solursh et al. 1981). In *Dbf* mutant limbs, the interdigital mesenchyme remains

thick for longer than that of wild type embryonic limbs, keeping the 2 inhibitory layers apart. We suggest that the preaxially enlarged *Dbf* limb bud is sufficient to support more than 5 condensations when the pattern is first laid down, further additions (interdigital condensations and bifurcations) being possible slightly later, due to the persistence of proliferative signals emanating from the retained interdigital AER and to the prolonged separation of the dorsal and ventral layers of ectoderm. It is also interesting that the digits in *Dbf* limbs do not all develop in the same plane, a phenomenon observed in human embryos with preaxial polydactyly (Yasuda, 1975).

Abnormalities of the tibia are also present in *Dbf* mutant fetuses. At d 15 the tibia can be seen to originate as 2 separate centres of chondrogenesis, rather than as a single cartilaginous model. By d 14 the proximal tibial cartilage has the characteristic appearance of hemimelic tibia (Karchinov, 1973); the resulting hypoplastic tibia causes a bowing of the fibula at later stages of fetal development. The medial placement of the articulation of the tibia with the talus leads to the clubfoot deformity that is easily recognisable in older fetuses and postpartum animals.

A number of causes for clubfoot have been proposed, the most favoured being intrauterine moulding, possibly as a result of oligohydramnios (Dunn, 1985). Dietz (1985) suggested that whereas postural clubfoot, which corrects itself within a few weeks of birth in human infants, may be brought about by mechanical factors such as oligohydramnios, noncorrecting clubfoot may have an underlying genetic component; the *Dbf* mutant mouse is a clear example of this. Although the manifestation of this defect is much less severe in the forelimbs, the radii and ulnae are in some animals slightly abnormal, and some of the animals exhibit a manus equinovarus deformity (clubhand), walking on the outer border of both fore and hind-feet.

The heads of the mutants are discernibly abnormal midway through gestation, with a distinctive bulge appearing in the roof of the diencephalon. This bulge corresponds with the position of the ectopic bone seen in the anterior fontanelle of older animals. Other skeletal elements of the cranium were seen to be enlarged also, and the calvarial bones of all of the mutant skulls were separated by wider than normal sutures. Although relatively common in humans, wormian bones (supernumerary bones of the skull vault) are not seen in the genetic background of the wild type strain used in this study (C3H/101). Homozygotes exhibited characteristic midline fusion defects of the face, in addition to the other defects that we report present in the heterozygous animals. Midline cleft face is an unusual defect, but has also been observed in severe vitamin A deficiency (Morriss-Kay & Sokolova, 1996) and in mice lacking 2 retinoic acid receptors (Lohnes et al., 1994). Elucidation of the mechanisms underlying craniofacial defects, including possible involvement of the retinoic acid signalling pathway, will be possible when the *Dbf* gene has been characterised.

In a previous study we have shown that the *Dbf* gene product is a novel component of an evolutionarily conserved signalling pathway, the *Shh* (Sonic hedgehog) signalling pathway (Hayes et al. 1998). *Shh* has been shown to be a key molecule involved in the establishment of pattern in the vertebrate limb along the anteroposterior and the proximodistal axes (Riddle et al. 1993; Laufer et al. 1994). The result of the mutation is the ectopic activation of this pathway throughout the distal mesenchyme of the developing mutant limb buds, so that polarising activity is widespread rather than being confined to a discrete ZPA at the posterior margin of the limb bud. At the molecular level, all the limb buds cells gain the character of posterior cells, resulting in the ectopic (anterior/preaxial) induction of molecular signals, including fibroblast growth factor 4 (Fgf4). Fgf4 secretion from the posterior AER is responsible for mesenchymal proliferation during limb bud outgrowth. Its ectopic expression in the anterior AER of *Dbf* limb buds is likely to be the stimulus for the preaxial mesenchymal proliferation that must underlie the expansion of tissue seen at late d 10/early d 11, and of the later interdigital mesenchymal proliferation when the AER regression is delayed.

Interestingly, reports of the molecular characterisation of several other polydactylous mutants differ from *Dbf* in that these mutants have been shown to possess a second (anterior) polarising region, as visualised by the ectopic expression of *Shh* (Chan et al. 1995, Masuya et al. 1995, 1997). Morphologically, this manifests itself as the presence of 1 or 2 supernumerary digits, in a partial mirror-image pattern. In contrast, *Dbf* limbs show normal *Shh* expression, but polarising activity and activation of the *Shh* pathway is uniform throughout the mesenchyme of the mutant limbs (Hayes et al. 1998). This uniformity of *Shh* pathway activation explains the lack of anteroposterior polarity in the mutant limb, in which all the digits are triphalangeal.

Mutations in the currently identified components of the murine *Shh* signalling pathway have all yielded limb phenotypes. Furthermore, mutations in the transcription factor *GLI*3 has been shown to be

responsible for Greig cephalopolysyndactyly syndrome in man, affecting the limbs and craniofacial region (Hui & Joyner 1993). Human mutations in the other elements of the pathway, *SHH* and *PTC*, have also given phenotypes reminiscent of those seen in mouse (Chiang et al. 1996; Goodrich et al. 1997). Polysyndactyly with interdigital cartilaginous elements has been observed in mice lacking both alleles of *Hoxd13* and 1 allele of *Hoxa13* (Fromental-Ramain et al. 1996). All of these mutations involve genes that are primary or secondary targets of *Shh* signalling. Overexpression of *Shh* itself causes the development of limbs with ectopic interdigital elements and digital bifurcations (Oro et al. 1997).

The mouse mutant *Dbf* therefore represents a means to investigate not only the interactions of the *Shh* signalling pathway, but also represents a fundamental model to understand human dysmorphogenetic syndromes involving the limbs and head. The *Dbf* locus maps to mouse chromosome 1 in a region of conserved synteny with the long arm of human chromosome 2 (Lyon et al. 1996*a*; Lyon & Kirby, 1996*b*). Interestingly, this region of the human chromosome harbours 2 loci for brachydactyly (Dean, 1996), which is the reduction, or absence, of some or all of the distal limb elements. This phenotype is what would be predicted for a loss of function allele of the human *DBF* gene, based on our observations in the mouse (Lyon et al., 1996*a*; Hayes et al. 1998; this report), raising the possibility that the *Dbf* gene is a murine orthologue of the human gene at one of the *Brachydactyly* loci.

ACKNOWLEDGEMENTS

We thank Martin Barker for technical assistance, Sue Morse for animal care and Youichirou Ninomiya for Figure 6*a*. CH is in receipt of a studentship from the Anatomical Society of Great Britain and Ireland; MFL was partly supported by EU contract no. CHRX-CT93–0181. The animal stocks at Harwell were maintained under the guidance issued by the Medical Research Council and Home Office project licence no. 30/00875.

REFERENCES

Chiang C, Litingtung Y, Lee E, Young KE, Cordoen JL, Westpal H et al. (1996) Cyclopia and axial patterning in mice lacking Sonic hedgehog gene function. *Nature* **383**, 407–413.

Chan DC, Laufer E, Tabin C, Leder P (1995) Polydactylous limbs in Strong's Luxoid mice result from ectopic polarizing activity. *Development* **121**, 1971–1978.

Dean, M (1996) Polarity, proliferation and the *hedgehog* pathway. *Nature Genetics* **14**, 245–247.

Dietz, FR (1985) On the pathogenesis of clubfoot. *Lancet* 388–390.

Dunn, PM (1985) Pathogenesis of clubfoot. *Lancet* 635–636.

Fromental-Ramain C, Warot X, Messadecq N, Lemeur M, Dolle P, Chambon P (1996) *Hoxa*-13 and *Hoxd*-13 play a crucial role in the patterning of the limb autopod. *Development* **122**, 2997–3011.

Goodrich LV, Milenkovic L, Higgins KM, Scott MP (1997) Altered neural cell fates and medulloblastoma in mouse *patched* mutants. *Science* **277**, 1109–1113.

Hayes C, Brown JM, Lyon MF, Morriss-Kay GM (1998) *Sonic hedgehog* is not required for polarisinig activity in the *Doublefoot* mutant mouse limb bud. *Development* **125**, 351–357.

Hui CC, Joyner AL (1993) A mouse model of greig cephalopolysyndactyly syndrome: the *extra-toes*^{J} mutation contains an intragenic deletion of the *Gli3* gene. *Nature Genetics* **3**, 241–246.

Hurle JM, Ganan Y, Macias D (1989) Experimental analysis of the *in vivo* chondrogenic potential of the interdigital mesenchyme of the chick leg bud subjected to local ectoderm removal. *Developmental Biology* **132**, 368–374.

Karchinov K. (1973) Congenital diplopodia with hypoplasia or aplasia of the tibia. *Journal of Bone and Joint Surgery* **55B**, 604–611.

Laufer E, Nelson CE, Johnson RL, Morgan BA, Tabin C (1994) *Sonic hedgehog* and *Fgf-4* act through a signaling cascade feedback loop to integrate growth and patterning of the developing limb. *Cell* **79**, 993–1003.

Lyon MF, Quinney R, Glenister PH, Kerscher S, Guillot P, Boyd Y (1996*a*) Doublefoot: a new mouse mutant affecting development of limbs and head. *Genetical Research* **68**, 221–231

Lyon MF, Kirby, MC (1996*b*) Mouse chromosome atlas. In *Genetic Variants and Strains of the Laboratory Mouse*, 3rd edn (ed Lyon MF, Rastan S, Brown SDM), pp 881–923. Oxford: Oxford University Press.

Lohnes D, Mark M, Mendelsohn C, Dolle P, Dierich A, Gorry P et al. (1994). Function of the retinoic acid receptors (RARs) during development (I) Craniofacial and skeletal abnormalities in RAR double mutants. *Development* **120**, 2723–2748.

Masuya H, Sagai T, Wakana S, Moriwaki K, Shiroishi T (1995) A duplicated zone of polarizing activity (ZPA) in polydactylous mouse mutants. *Genes and Development* **9**, 1645–1653

Masuya H, Sagai T, Moriwaki K, Shiroishi T (1997) Multigenic control of the localization of the zone of polarizing activity in limb morphogenesis in the mouse. *Developmental Biology* **182**, 42–51

Morriss-Kay GM, Sokolova NV (1996) Embryonic development and pattern formation. *FASEB Journal* **10**, 961–968.

Niswander L, Tickle C, Vogel A, Booth I, Martin GR (1994) FGF-4 replaces the apical ectodermal ridge and directs outgrowth and patterning in the vertebrate limb. *Cell* **75**, 579–587.

Oro AE, Higgins KM, Hu Z, Bonifas J, Epstein EH Jr, Scott MP (1997) Basal cell carcinomas in mice overexpressing Sonic hedgehog. *Science* **276**, 817–821.

Riddle RD, Johnson RL, Laufer E, Tabin C (1993) Sonic hedgehog mediates the polarizing activity of the ZPA. *Cell* **75**, 1401–1416.

Saunders JW (1948) The proximo-distal sequence of origin of limb parts of the chick wing and the role of ectoderm. *Journal of Experimental Zoology* **108**, 363–404.

Saunders JW, Gasseling MT (1968) Ectodermal-mesenchymal interactions in the origin of symmetry. In *Epithelial–Mesenchymal Interactions* (ed. Fleischmajer, R, Billingham, RE), pp.78–97. Baltimore: Williams and Wilkins.

Savage MP, Hart CE, Riley BB, Sasse J, Olwin BB, Fallon, JF (1993) Distribution of FGF-2 suggests it has a role in chick limb bud growth. *Developmental Dynamics* **198**, 159–170.

Solursh M, Singley CT, Reiter RS (1981) The influence of epithelia on cartilage and loose connective tissue formation by limb mesenchyme cultures. *Developmental Biology* **86**, 471–482.

Summerbell D, Lewis J, Wolpert L (1973) Positional information in chick limb morphogenesis. *Nature* **224**, 492–496.

Tickle C, Eichele G (1994) Vertebrate limb development. *Annual Review of Cell Biology* **10**, 121–152.

Watson AG (1977) In toto alcian blue staining of the cartilaginous skeleton in mammalian embryos. *Anatomical Record* **187**, 743.

Wilkie AOM, Morriss-Kay GM, Jones EY, Heath JK (1995) Functions of fibroblast growth factors and their receptors. *Current Biology* **5**, 500–507.

Winter RM (1994) Clinical syndromes with combined cranial and limb defects. *Seminars in Developmental Biology* **5**, 275–281.

Yasuda M (1975) Pathogenesis of preaxial polydactyly of the hand of human embryos. *Journal of Embryology and Experimental Morphology* **33**, 745–756.